Dalton Transactions

Accepted Manuscript

ROYAL SOCIETY OF CHEMISTRY

www.rsc.org/dalton

Journal Name

RSCPublishing

COMMUNICATION

Intramolecular Excimer Formation in Hexakis(pyrenyloxy)cyclotriphosphazene: Photophysical Properties, Crystal structure, and Theoretical Investigation

Cite this: DOI: 10.1039/x0xx00000x

Received 00th January 2012,
Accepted 00th January 2012

DOI: 10.1039/x0xx00000x

www.rsc.org/

Serkan Yeşilot[a*], Bünyemin Çoşut[a], Hüsnüye Ardıç Alidağı[a], Ferda Hacıvelioğlu[a], Gül Altınbaş Özpınar[b**], Adem Kılıç[a]

Abstract

A hexakis(pyrenyloxy)cyclotriphosphazene is synthesized by the reaction of $N_3P_3Cl_6$ with 2-hydroxypyrene and its excimer emission through intramolecular interactions in solution and in the solid state has been investigated by the fluorescence spectroscopy and X-ray crystallography. Thermal and electrochemical properties were investigated. A DFT benchmark study has been performed to evaluate the intramolecular interactions and molecular orbital levels by comparing with the experimental results.

Excimer emissions through π-stacking interactions based on conformationally rigid aromatic systems have been attracting interest in the field of organic molecular electronics. For examples, excimer emission arising from *intra-* or *intermolecular* π---π stacking interactions have been widely studied for organic light emitting devices (OLEDs).[1] Pyrene excimer formation is a well-known concentration-dependent phenomenon in organic solutions[2] and its excimer emission has been successfully employed in solutions for many applications such as chemical sensors, biological probes, etc. [3] However, the use of pyrene in solid-state media as light emitting materials in electroluminescent devices has been limited due to two main drawbacks; the first one is the pyrene molecules have a high propensity towards strong *intermolecular* interactions in the solid state, which leads to an additional emission band in long wavelength and the quenching of fluorescence resulting in low solid-state fluorescence quantum yields. [4] The other is that pyrene exhibits the absorption and emission wavelengths of approximately 310 and 380 nm, respectively, so as not to cover the desired light emitting region. [5] These problem are mainly solved by the development of various synthetic strategies, which are mostly included in the extended π- conjugation systems by introducing poly aromatic hydrocarbons (e.g, phenylene, naphthalene, pyrene, thiophene, fluorene, carbazole, etc).[6] However, designing and synthesis of the conformationally rigid pyrenyl systems have attracted considerable attention in recent years due to their strong π---π stacking interactions which could suppress the undesirable additional emission and/ or aggregation in the solid state. For examples, there have been reported the highly sterically hindered tetrasubstituted pyrene derivatives [7] which can emit blue light in solution as well in the solid state and with high quantum yield. There have also been recent reports on excimer emission from intramolecular strong π---π interactions in pyrene-naphthalene [1e] and pyrene-calixarene [1g] derivatives and their application in OLEDs. However, most of light-emitting conformationally rigid systems are generally synthesized by more complicated processes involving sequential reactions with low yields. Therefore, it is still important to consider the synthesis of the π-stacked molecules by using simple, rapid and inexpensive methods. Moreover, synthesised rigid systems are mostly small molecules in nature, whereas dendrimers have more advantages which include the properties of both small molecules and polymers for application in OLEDs.[8b,c and d]

In this contribution a conformationally rigid molecule is synthesized from commercially available starting materials (hexachlorocyclotriphosphazene and 2-hydroxpyrene) in only one-step reaction with high yield. Hexakis(pyrenyloxy)cyclotriphosphazene **(HPCT)** exhibited an intramolecular excimer emission arising from the non-covalent π---π and CH---π stacking interactions among the pyrenyloxy moieties

which were investigated by the fluorescence spectroscopy, X-ray crystallography, and as well as theoretical simulation.

Commercially available hexachlorocyclotriphosphazene, $N_3P_3Cl_6$, was selected as the core, due to its fascinating properties, such as high thermal stability and extremely susceptible to nucleophilic reactions under basic conditions, thus allowing to prepare a variety of cyclotriphosphazene-based dendrimers.[8] Besides, when trimer is fully substituted with identical aryloxy substituents, the structural rigidity of cyclotriphosphazene ring leads to a preferred conformation in which the three aryloxy substituents on either side of the cylic core are approximate reciprocally equidistant. This conformational property is crucial in this work because it may allow the *intramolecular* π---π interactions among the attached aryloxy groups, if the appropriate aryloxy units are chosen. For examples, when fully substituted hexakis(aryloxy)cyclotriphosphazene was derived from simple phenol [9a], it was seen that there was no any *intramolecular* π---π intraction between phenol rings. For naphthyloxy derivative, it was found [9b] that the distance between the naphthol rings is 4.5 Å which is almost limit value for an ideal distance for *intramolecular* π---π interaction. Hence, hydroxpyrene was chosen as a large chromophore group, and hexakis(pyrenyloxy)cyclotriphosphazene **(HPCT)** easily obtained from a nucleophilic displacement reaction of hydroxypyrene with trimer ,$N_3P_3Cl_6$, under argon atmosphere with cesium carbonate as base in 83% yield (Fig.1 a). **HPCT** was characterized by the standard spectroscopic techniques such as ^1H and ^{31}P NMR, mass spectrometry (MALDI-TOF), and elemental analysis. All the results were consistent with the predicted structure as shown in the supplementary information (see experimental section and Fig. S1-S3).

Fig. 1.

Chlorophosphazenes ($N_3P_3Cl_6$, or $N_4P_4Cl_8$) are photochemically inactive and do not interfere with the photophysical properties of the attached chromophores. Hence, it would be expected that absorption and emission spectra of **HPCT** could be similar compared to the attached pyrenyloxy groups. The absorption spectra of **HPCT** and hydroxypyrene in dilute dichloromethane solutions were displayed in Fig. 2a. Apart from intensity differences reflecting the number of pyrenyloxy groups, the both spectra are almost identical with related to absorption spectrum of hydroxypyrene. The similarity of UV spectra indicates that there is no effective ground state interaction among the pyrenyloxy groups. In contrast, the fluorescence emission spectra of **HPCT** and hydroxypyrene are significantly different. The hydroxypyrene exhibited common pyrene-like florescence emission with a maximum wavelength at 386 nm in dichloromethane with dilute solutions of $2x10^{-7}$ mol.dm^{-3} (Fig 2b). Whereas the fluorescence emission of **HPCT** appeared at 459 nm in dichloromethane with same concentration, and displayed red-shifted emission wavelengths of up to 73 nm when compared to the hydroxypyrene emission. Although this red-shifted emission is very similar to the characteristic *intermolecular* pyrene excimer emission in high concentration solution, it is well known that pyrene itself does not exhibit excimer emission at concentrations of 10^{-7} M and below. [10] Therefore, we conclude that significant *intramolecular* excimer emission occurs among the attached pyrenyloxy groups. The observed excimer emission was consistent with previous other hexakis aryloxy phosphazene research papers.[8a,e,11] The fluorescence emission spectra of the **HPCT** was recorded in the solvents of different polarity such as cyclohexane, 1,4-dioxane, tetrahydrofuran (THF), toluene, dichloromethane, acetonitrile, methanol and water with dilute solutions of $5x10^{-7}$ mol.dm^{-3} (Fig. S4). The spectrum obtained in cyclohexane was very similar to the that in dichloromethane. The spectra obtained in THF, 1,4-dioxane and toluene showed excimer emission bands consisting of maxima at around 440 nm and 460 nm, together with two shoulders at 383 nm and 405 nm which are belong to monomer pyrene emission. On the contrary, the spectra obtained in more polar solvents (water, methanol and acetonitrile) showed only monomer pyrene emission and disappeared the excimer emission. This negative solvatochromism has been observed in previously reported pyrenyl systems, and probably due to the disruption of the π-stacking interactions in more polar solvents. [12] In addition, **HPCT** showed fluorescence emission in the solid state as well (Fig.2b). The spectrum is very similar to dilute solutions spectrum, and exhibits a small red shift (approximately 7 nm) at the maximum wavelength, suggesting that there is little change in molecular conformation from the solution to the solid state for **HPCT.** This result, showing very similar emission spectra both in dilute solution and solid state is evidence that the intermolecular aggregation is almost suppressed due to the molecular arrangement of the pyrenyloxy units on cyclotriphosphazene ring. Furthermore, Fig. S5 showed the identical emission spectra obtained for a **HPCT** before and after annealing at 200 °C for 24 h under argon atmosphere, resulting that the molecular conformation was stable at high temperature.

Fig.2.

The thermal stability of **HPCT** was evaluated using thermogravimetric analysis (TGA) and differential scanning calorimetry (DSC). **HPCT** exhibited high thermal decomposition temperature (T_d) at 443°C (corresponding to 5% weight loss, see Fig. S6) and morphologically stable amorphous material with glass transition temperature (T_g) at 137 °C (Fig. S7), all of which are desired properties for the application in light emitting electroluminescence devices.

Electrochemical properties of **HPCT** were investigated by cyclic voltammetry. The electrochemical data are obtained from the oxidation and reduction cyclic voltammograms as shown in Fig. S8. The HOMO energy level of **HPCT** was calculated using the equation: HOMO = -[Eox - E1/2(ferrocene) + 4.8] V, where Eox is the onset oxidation potential of and E1/2(ferrocene) is the onset oxidation potential of ferrocene vs. Ag/Ag++. The band gap (Eg) was calculated from the onset absorption edge in the UV-vis spectrum of HPCT and found to be 3.45 eV, and then the LUMO can be estimated to be -3.03 eV. The obtained electrochemical values, which are very similar to previously, reported studies [13] could be acceptable to fabricate an electroluminescent device.

HPCT is largely amorphous. After trying several solvents and solvent combinations, only poorly diffracting crystal was

obtained from dichloromethane. Crystallographic data and refinement details of the data collection for **HPCT** are given in Table S1.Single crystal X-ray analysis of **HPCT** showed that the six-pyrenyloxy groups lie almost perpendicularly above and below the nearly planar cyclotriphosphazene core (Fig. 1b). Fig. 3 shows the selected intramolecular π—π interactions among pyrenyloxy units as well as a number of CH—π interactions. The distance for *intramolecular* π—π interaction between two face-to-face prenyloxy groups is in the range of 3.399(9) to 3.607(9) Å, which is within the range of the typical distance for π-π interaction (3.5 Å). The distance for *intramolecular* CH—π interactions among the pyrenyloxy moieties is in the range of 2.74 [with D—A distance of 3.367(16)] to 2.88(with D—A distance of 3.708(16)] Å and all data summarized in Table S2 and S3. In addition, crystal structure analysis of **HPCT** allowed seeing the *intermolecular* π-stacking interactions between the molecules (see Fig S9), which may be attributed to a small red shift of its emission spectrum in solid state (Fig 2b).

Fig.3.

To gain further information about molecular interaction and energy levels of **HPCT**, we have performed theoretical computations using density functional theory (DFT). We first performed a benchmark study on the noncovalent intramolecular interaction and determination of energy levels of molecular orbitals because of two reasons: One of the reasons is that many functionals are generally far from the targeted chemical accuracy due to their inherent methodological problems.[14] The other one is that experimentally computed HOMO-LUMO gap shows discrepancy with respect to the measurement techniques used (3.45 eV determined from the onset of UV-Vis absorption spectra and 2.59 eV from the cyclic voltammetry). Geometry optimizations were performed using the most popular DFT method, B3LYP and Truhlar's functional MPW1B95 with 6-31G(d) basis set, which are recommended computing band gap and describing noncovalent interactions, respectively [15], and also using Grimme's functional including dispersion, B97D with 6-31G(d) basis set and recently developed functionals which account for long-range correction such as CAM-B3LYP, LC-wPBE, and wB97XD using cc-pVDZ basis set. HOMO-LUMO gap and the first vertical excitation energy were computed by performing single point time-dependent DFT (TD-DFT) calculations at the same levels and using TD-B97D/TZVP level due to that Huenerbein and Grimme's study [16] indicates that the combination of TD-DFT method with high- exchange hybrid functionals and the dispersion corrected DFT (DFT-D) can describe interacting systems with adequate accuracy.There have been some reports of the computational studies of the aryloxy cyclic phosphazenes, which were mostly derived from phenol or its derivatives.[17] To our best knowledge, our DFT calculations are the first detailed study on chemistry of hexakis(aryloxy)cyclotriphosphazene using a large group.

Noncovalent intramolecular interactions in the **HPCT** structure are demonstrated in Figure S10 and tabulated in Table S2 and S3. According to single crystal X-ray analysis of **HPCT**, interacting pyrene rings shows a parallel-displaced structure. All DFT methods studied, except from CAM-B3LYP and B3LYP methods, find the same parallelism. Nevertheless, CAM-B3LYP/cc-pVDZ and B3LYP/6-31G(d) levels fail to describe intramolecular interactions by producing geometries in which two prenyloxy groups bound to same phosphorus atom are almost perpendicular (Fig. S11). Failure of B3LYP can be attributed to the lack of range separated exchange-correlation functionals, but intriguing point is that long-range corrected CAM-B3LYP functional also exhibited poor performance.

π---π interaction distances obtained from X-ray analysis varies in the range of 3.399(9)-3.607(9)Å (Table S2 and Figure S3). The distances calculated with wB97XD/cc-pVDZ, B97D/6-31G(d) and MPW1B95/6-31G(d) agree well with the experimental results and the findings obtained from theoretical investigations on pyrene dimer performed by Huenerbein and Grimme [15] and Kolaski and coworkers [18] whereas LC-wPBE/cc-pVDZ overpredicts the π---π interaction distances. For C-H---π interactions, wB97XD/cc-pVDZ and B97D/6-31G(d) underestimate interaction distances while LC-wPBE/cc-pVDZ and MPW1B95/6-31G(d) overestimate. Fig.4 shows mean unsigned errors (MUEs) of DFT methods studied (except for B3LYP and CAM-B3LYP) in the estimation of interaction distances. Although LC-wPBE/cc-pVDZ optimization leads to a consistent geometry with experimental one, the calculated MUEs are 0.656 and 0.360 Å for π---π and C-H---π interactions, respectively. The wB97XD/cc-pVDZ level exhibits the best performance (MUE is 0.100 Å for π---π and 0.065 Å for C-H---π interactions). On the other hand, this level requires very high computing effort for large systems such **HPCT**. B97D and MPW1B95 with 6-31G(d) provide adequate accuracy for the estimation of noncovalent intramolecular interactions. MPW1B95 (MUE of 0.135 Å) is even slightly better than B97D (MUE of 0.165 Å) for π---π interactions. Many studies in literature verify that MPW1B95 exhibits excellent performance for nonbonded interactions .[15,19, 20]

Fig. 4.

Table S4 shows the experimental and calculated molecular orbital energies. Functionals including long-range correction such as CAM-B3LYP, LC-wPBE and wB97XD with cc-pVDZ basis set highly overestimated the HOMO-LUMO gaps. Single point TD-DFT computations on the X-ray geometry show that B3LYP functional agree well with the optical band gap (with an error of 0.08-0.09 eV) and improving basis set does not dramatically alter the energies. On the other hand, HOMO-LUMO gap computed with TD-B97D/TZVP level is consisted with the result obtained from cyclic voltammetry experiment. E_g value obtained from MPW1B95/6-31G(d) optimization is 0.47 eV higher than the optical band gap whereas single point TD-B3LYP/6-31G(d) computation on the MPW1B95/6-31G(d) geometry produces lower energy by 0.12 eV. Besides, TD-B97D/TZVP// MPW1B95/6-31G(d) underestimates the E_g by 0.39 eV relative to the result of cyclic voltammetry experiment. HOMO-LUMO gap computed from B97D/6-31G(d) optimization is 1.98 eV, which is lower than the result of cyclic voltammetry experiment by 0.61 eV. Single point TD-B97D/TZVP computation on the B97D/6-31G(d) geometry increases this value by only 0.02 eV.

From the molecular orbital computations, the conclusion that can be drawn is that single point B97D/TZVP computations on

either experimental or optimized geometry produce similar results (2.00 – 2.38 eV) to cyclic voltammetry experiment result (2.59 eV) but B3LYP/6-31G(d) gives resemble values (3.33 – 3.53 eV) to the optical band gap (3.45 eV). However, there is difference between the experimental gaps by 0.86 eV. The selection of which DFT method gives the most accurate energy should be based on the differences between experiments of UV-vis and CV in the determination of HOMO-LUMO gap. The optical band gap calculated from UV-vis experiment is considered an approximation noting the difference between HOMO and LUMO levels but providing no description of their actual levels. Furthermore, during the UV-vis operation and measurement, maximum absorbance wavelength can be affected by several factors such as solvent, temperature and concentration of the observed sample, which can vary the optical band gap. [21] However, cyclic voltammetry consisting of cycling a controlled potential across two electrodes and measuring resulting current provides the determination of oxidation and reduction potentials of the sample which allows the computations of HOMO and LUMO energies. Therefore, based on the CV experiment, B97D/TZVP level performs best among the DFT methods used in the estimation of HOMO-LUMO gap.

The first vertical excitation energies computed from single point TD-DFT calculations are also tabulated in Table S4. TD-CAM-B3LYP and TD-wB97XD with cc-pVDZ basis set slightly overestimates excitation energy by 0.43 and 0.27 eV, respectively with respect to optical band gap but the energy calculated with LC-wPBE is still considerably high. Comparing the computed excitation energies with the calculated HOMO-LUMO gap, TD-B3LYP method with 6-31G(d) and 6-31G+(d) basis sets shows a decrease of 0.44 eV whereas TD-B97D/TZVP level finds the same energy with E_g which agrees well with the energy computed from CV experiment. This supports that single point TD-B97D/TZVP computation on experimental or optimized geometry produces very accurate results in the determination of molecular orbital and excitation energies. HOMO-LUMO orbitals of **HPCT** are shown in Fig.5. HOMO orbital consists of only π-electron clouds of parallel displaced pyrene dimer and shows similarity with that of Huenerbein and Grimme. [16]

Fig. 5.

To summarize, a conformationally rigid molecule was presented with many advantages for light emitting materials in electroluminescent devices including one- step-high yield reaction, high thermal stability, high glass-transition temperatures (T_g), and high solubility in common organic solvents. Furthermore, its three-dimensional scaffold structure suppressed the pyrene aggregation in solid state due to intramolecular forces among pyreneoxy units as confirmed by experimental and theoretical studies. According to the preliminary results, this material appears to be promising candidate for blue-emitting OLEDs.

Acknowledgements

We wish to thank TÜBİTAK (Project Number; TBAG-110T142) for financial support. We also thank TUBITAK ULAKBIM, High Performance and Grid Computing Center (TR-Grid e-Infrastructure) for the calculations reported in the theoretical part of this paper.

[a] *Department of Chemistry, Gebze Institute of Technology, P.O.Box: 141, Gebze 41400, Kocaeli, Turkey, e-mail : yesil@gyte.edu.tr Tel: 00 90 262 6053137 Fax: 00 90 262 6053101*

b Department of Chemistry Technology, Biga Vocational School, Çanakkale Onsekiz Mart University, Biga 17200 Çanakkale, Turkey; e-mail:galtinbas@gmail.com, gul.ozpinar@comu.edu.tr Tel: 00 90 286 3162878 Fax: 00 90 286 3163733

Electronic Supplementary Information (ESI) available: Experimental procedures, additional figures and tables, X-ray crystallographic information, computational details in company with references, the optimized Cartesian coordinates and absolute energies of all stationary points. CCDC 965728 contains the supplementary crystallographic data for **HPCT** and can be obtained free of charge from The Cambridge Crystallographic Data Centre via www.ccdc.cam.ac.uk/data_request/cif. For ESI data in electronic format see DOI: 10.1039/c000000x/

1 *(a)* M. Mazzeo, V. Vitale, F. Della Sala, M. Anni, G. Barbarella, L. Favaretto, G. Sotgiu, R. Cingolani and G. Gigli, *Adv. Mater*., 2005, **17**, 34; *(b)* Y. Liu, M. Nishiura, Y. Wang and Z. Hou, *J. Am. Chem. Soc*., 2006, **128**, 5592; *(c)* S. Tao, Y. Zhou, C.-S. Lee, S.-T. Lee, D. Huang and X. Zhang, *J. Mater. Chem.*, 2008, **18**, 3981; *(d)* D. Thirion, M. Romain, J. Rault-Berthelot and C. Poriel, *J.Mater. Chem*., 2012, **22**, 7149; *(e)* J.-Y. Hu, Y.-J. Pu, G. Nakata, S. Kawata, H. Sasabe and J. Kido, *Chem. Commun*., 2012, 48, 8434; *(f)* J.-Y. Hu, Y.-J. Pu, Y. Yamashita, F. Satoh, S. Kawata, H. Katagiri, H. Sasabe and J. Kido, *J. Mater. Chem. C*, 2013, **1**, 3871; *(g)* K. Chan, J.P Fong Lim, X. Yang, A. Dodabalapur, G. E. Jabbour, A. Sellinger, *Chem. Commun*., 2012, **48**, 5106.

2 *(a)* J. B. Birks, *Photophysics of Aromatic Molecules*, Wiley, London, 1970; *(b)* F. M. Winnik, *Chem. Rev*., 1993, **93**, 587.

3 *(a)* H. N. Kim, W. X. Ren, J. S. Kim and J. Yoon, *Chem. Soc. Rev*., 2012, **41**, 3210; *(b)* E.T. Kool, Acc. Chem. Res., 2002, 35, 936; *(c)* K. Yamana, T. Iwai, Y. Ohtani, S. Sato, M. Nakamura and H. Nakano, *Bioconjugate Chem.*, 2002, **13**, 1266.

4 *(a)* A. C. Grimsdale, K. L. Chan, R. E. Martin, P. G. Jokisz, A. B. Holmes, *Chem. Rev.*, 2009, **109**, 897; *(b)* M. Shimizu, H. Tatsumi, K. Mochida, K. Shimono, T. Hiyama, *Chem. Asian J*., 2009, **4**, 1289; *(c)* A. Iida, S. Yamaguchi, *Chem. Commun.*, 2009, 3002.

5 *(a)* T. Azumi, S.P. McGlynn, *J. Chem. Phys*., 1964, **41**, 3131; *(b)* E. Clar, W. Schmidt, *Tetrahedron*, 1976, **32**, 2563.

6. S. H. Ko, *Organic Light Emitting Diode – Material, Process and Devices*, Published by InTech, Croatia, Chapter 2, 2011.

7 *(a)* J. N. Moorthy, P. Natarajan, P. Venkatakrishnan, D. F. Huang and T. J. Chow, *Org. Lett.*, 2007, **25**, 5215; *b)* W. Sotoyama, H. Sato, M. Kinoshita, T. Takahashi, A. Matsuura, J. Kodama, N. Sawatari, H. Inoue, *SID Digest* 2003, **45**, 1294; *(c)* S. Z. Bisri, T. Takahashi, T. Takenobu, M. Yahiro, C. Adachi, Y. Iwasa, Jpn. *J. Appl. Phys.*, 2007, **46**, 596; (c) T. Oyamada, H. Uchiuzou, S. Akiyama, Y. Oku, N. Shimoji, K. Matsushige, H. Sasabe, C. Adachi, *J. Appl. Phys*., 2005, **98**, 074506; *(d)* H.-Y. Oh, C. Lee, S. Lee, *Org. Electron*., 2009, **10**, 163.

8 *(a)* B. Çoşut, S.Yeşilot, *Polyhedron*, 2012, **35**, 101; *(b)* H. J. Bolink, S. G. Santamaria, S. Sudhakar, C. Zhen, A. Sellinger, *Chem. Commun*, 2008, 618; *(c)* S. Sudhakar and A. Sellinger, *Macromol. Rapid Commun.*, 2006, **27**, 247; *(d)* H. J. Bolink, E. Barea, R. D. Costa, E. Coronado, S. Sudhakar, C. Zhen, A. Sellinger, *Organic Electronics*, 2008, **9**, 155; *(e)* J. Xu, C. L. Toh, K. L. Ke, J. J. Li, C. M. Cho, X. Lu, E. W. Tan, C. He, *Macromolecules*, 2008, **41**, 9624;

9 *(a)* W. C. Marsh, J. Trotter, *J. Chem. Soc. A* , 1971, 169; *(b)* G. Bandoli, U. Casellato, M. Gleria, A. Grassi, E. Montoneri, G. C. Pappalardo, *Z. Naturforsch., B:Chem.Sci*., 1989, **44,** 575.
10 I. B. Berlman, *Handbook of Fluorescence Spectra of Aromatic Molecules*; Academic Press: New York, 1965, p 173.
11 *(a)* M. Gleria, F Barigelletti, S. Dellonte, S. Lora, F. M. Into, P. Bortolus, *Chem. Phys.Letters*, 1981, **83**, 559; *(b)* N. Chattopadhyay, B. Haldar, A. Mallick, S. Sengupta, *Tetrahedron Lett*, 2005, **46**, 3089.
12 *(a)* J. Bodapati, H. Icil**,** *Photochem. Photobiol. Sci*., 2011, **10**, 1283; *(b)* G. Venkataramana, S. Sankararaman, *Org. Lett*., 2006, **8**, 2739; *(c)* G. Venkataramana, S. Sankararaman, *Eur. J. Org. Chem*., 2005, 4162.
13*(a)* P. Schrögel, M. Hoping , W.Kowalsky, A. Hunze , G. Wagenblast, C. Lennartz , P. Strohriegl, *Chem. Mater*., 2011, **23**, 4947; *(b)* C. Tang, F. Liu, Y.-J. Xia, J. Lin, L.-H. Xia, G.-Y. Zhong, Q.-L. Fan, W. Huang, *Organic Electronic*, 2006, **7**, 155; *(c)* K.R. Justin Thomas, N. Kapoor, M. N. K. Prasad Bolisetty, J. –H. Jou, Y.-L. Chen, Y.-C. Jou, *J. Org. Chem.*, 2012, **77**, 3921.
14 L. Goerigk, S. Grimme, *J. Chem. Phys.*, 2010, **132**, 184103.
15 A. S. Özen, *J. Phys. Chem. C*, 2011, **115**, 25007.
16 R. Huenerbein, S. Grimme, *Chem. Phys*. 2008, **343**, 362.
17 *(a)* G. Gahungu, B. Zhang, J. Zhang, *Chem. Phys.Letters*, 2004, **388**, 422. *(b)* V.L. Furer, I.I. Vandyukova , A.E. Vandyukov , S. Fuchs , J.P. Majoral , A.M. Caminade , V.I. Kovalenko , J. Mol. Struct, 2009,**932**,97.*(c)* V.L. Furer, I.I. Vandyukova , A.E. Vandyukov , S. Fuchs , J.P. Majoral , A.M. Caminade , V.I. Kovalenko J. Mol. Struct., 2011,**1005**, 25. *(d)* V.L. Furer , I.I. Vandyukova , C. Padie , J.P. Majoral , A.M. Caminade b, V.I. Kovalenko, Chem. Phys., 2006,**330**, 349.
18 M. Kołaski, C. R. Arunkumar, K. S. Kim, *J. Chem. Theo. Comp*., 2013, **9**, 847.
19 Y. Zhao, D. G. Truhlar, *J. Chem. Theo. Comp*., 2005, **1**, 415.
20 Y. Zhao, O. Tishchenko, D. G. Truhlar, *J. Phys. Chem. B,* 2005, **109**, 19046.
21 K. Shelton, *New Photovoltaic Acceptors: Synthesis and Characterization of Functionalized C-Fused Anthradithiophene Quinones*, Master Thesis, University of Kentucky, 2011.

Figure Captions

Fig. 1. a) Synthetic pathway of **HPCT** and **b**) molecular structure of **HPCT** (hydrogens are omitted for clarity).

Fig.2. a) UV-vis spectra of **HPCT** and **1-hydroxypyrene** in dichloromethane b) Fluorescence emission spectra of (A) hydroxypyrene (B) **HPCT** in solution (C) **HPCT** in solid state.

Fig.3. Intramolecular π-π and C-H—π interactions in the structure of **HPCT**.

Fig. 4. Mean Unsigned Errors (MUEs) of DFT methods studied in the estimation of interaction distances.

Fig. 5. HOMO-LUMO orbitals of **HPCT** computed with TD-B97D/TZVP//MPW1B95/6-31G(d) level.

Figures

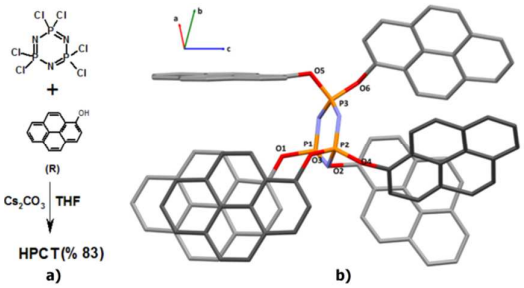

Fig. 1.

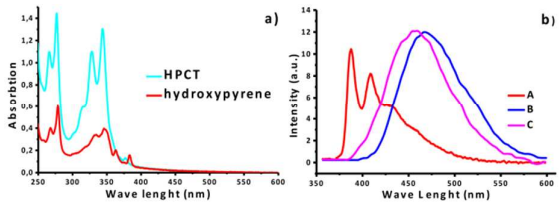

Fig.2.

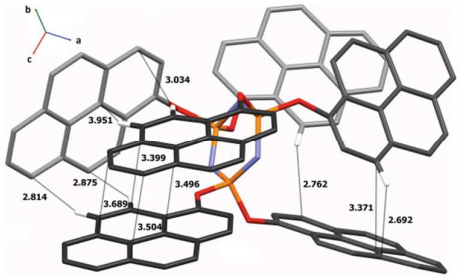

Fig.3.

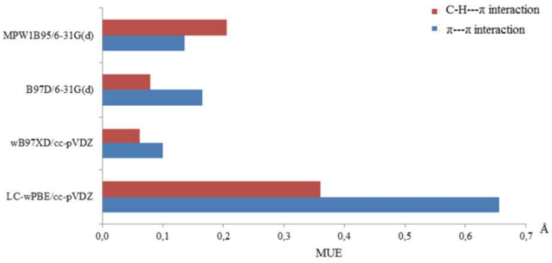

Fig.4.

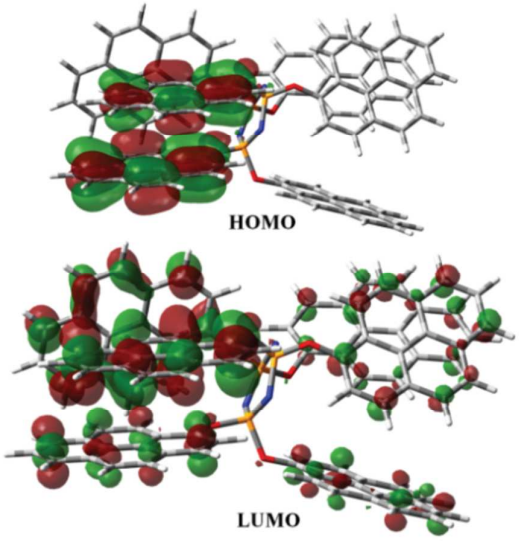

Fig. 5.